PENSOFT.

MUSEUM FÜR
NATURKUNDE
BERLIN

# Novel integrative data for two *Milnesium* Doyère, 1840 (Tardigrada: Apochela) species from Central Asia

Witold Morek[1], Bartłomiej Surmacz[1], Łukasz Michalczyk[1]

1  *Institute of Zoology and Biomedical Research, Faculty of Biology, Jagiellonian University, Gronostajowa 9, 30-387 Kraków, Poland*

*http://zoobank.org/8E352F18-23C9-4A13-BE12-92E30C3B95BF*

Corresponding author: Witold Morek (wmorek@op.pl)

## Abstract

Tardigrada are a phylum of microscopic animals inhabiting a variety of ecosystems, both aquatic and terrestrial, being recognised for their remarkable abilities to withstand tough environmental conditions. The order Apochela groups exclusively carnivorous species, with the vast majority representing the genus *Milnesium* Doyère, 1840. Representatives of this genus are characterised by simplified morphology, therefore possessing an extremely limited set of taxonomically meaningful morphological traits. Nevertheless, the taxonomy of *Milnesium* is mostly based on classical data: observations and measurements in light microscopy with the majority of descriptions lacking integrative data, most importantly DNA barcodes, but also scanning electron microscopy photographs and developmental variability analysis. Hence, re-descriptions that include novel integrative data are urgently needed. In this contribution, we provide new taxonomic data for two species described from Central Asia, *Milnesium almatyense* (a single population) and *Milnesium reductum* Tumanov, 2006 (five populations): morphometrics, DNA barcodes, SEM observations and description of developmental variability. As a result, we amend the description of both species and reveal phylogenetic relationships of those species and other sequenced congeners. The integrative data confirm the validity of the two species and include them in the growing set of *Milnesium* species associated with DNA sequences.

## Key Words

## Introduction

Tardigrades, commonly named as water bears, are a phylum of cosmopolitan invertebrates, inhabiting almost all environments across the world (Nelson et al. 2018). Currently around 1300 tardigrade species are recognised (Degma et al. 2009–2019) with 44 belonging to the order Apochela Schuster et al., 1980 which is characterised by a set of unique traits, i.e. a separation of the primary and secondary claw branches or the presence of peribuccal lamellae. Additionally, in contrast to parachelans, apochelans lack important morphological characters commonly utilised in their taxonomy, for example, placoids and septulum in the muscle pharynx or ornamented egg shells. The great majority of extant species (41 of 44) within the family Milnesiidae Ramazzotti, 1962, the only one in order

Apochela, are classified within genus *Milnesium* Doyère, 1840 (37 listed in Degma et al. 2009–2019, excluding two *nomina dubia*: *M. dujiangensis* and *M. tardigradum trispinosa*, but with a further four taxa described later on by Kaczmarek et al. 2019, Moreno-Talamantes et al. 2019, and Surmacz et al. 2019). Due to the limited number of taxonomically meaningful traits the classification of this genus is challenging and, so far, has been based mostly on classical morphological data that were shown to be at least partially insufficient in resolving the taxonomy of these tardigrades, as pseudocryptic species have recently started to be recognised (e.g. Morek et al. 2016a; Morek et al. 2019a; Surmacz et al. 2020). Moreover, it has been demonstrated that some *Milnesium* species exhibit developmental variability, in which the immature life stages, i.e. hatchlings and juveniles (1st and 2nd instar, respectively; Morek et al.

2019b) may exhibit different morphologies than the adults (3rd instar onwards), for example, in the number of points on secondary branches of claws (so called claw configuration, CC; Michalczyk et al. 2012a, b), dorsal cuticle sculpturing or buccal tube morphology (Morek et al. 2016a; Morek et al. 2019b; Morek et al. in press).

So far, the tardigrade fauna of Kazakhstan and Kyrgyz Republic have not been thoroughly investigated, with only a few contributions published in the current century, focusing mostly on descriptions of new species (e.g.: Tumanov 2003, 2005, 2006, 2007; Kaczmarek et al. 2018; Zawierucha et al. 2018 or Coughlan et al. 2019). In this region, three *Milnesium* species were described and two of them, *M. almatyense* Tumanov, 2006 and *M. reductum* Tumanov, 2006, are characterised by rare morphological traits: the [2-3]-[2-2] CC (*M. almatyense*) and the lack of accessory points (*M. reductum*). Although the descriptions are accurate and detailed, they lack the integrative data, such as scanning electron microscope imaging, information on ontogenetic variability and, most importantly, DNA sequences. Additional phenotypic data and genetic data for these species are needed, not only to aid their identification and to test against potential synonymies, but also to pinpoint the phylogenetic positions of both taxa. The phyletic relationships of *M. almatyense* and *M. reductum* are particularly interesting because of the rare phenotypic traits mentioned above. Specifically, in the first extensive phylogeny of *Milnesium* in Morek and Michalczyk (2020) only two species with a [2-3]-[2-2] CC and no species without accessory points were included.

Thus, the aim of this study was to collect integrative data for two species, *M. almatyense* and *M. reductum*, based on the material collected in the proximity of their *loci typici* in Kazakhstan and Kyrgyz Republic, respectively. The integrative analysis of six populations of the two species provided novel morphological and developmental traits and DNA barcodes, amending the descriptions of these taxa and allowed us to identify their kin.

## Materials and methods

### Sampling and specimens

We analysed six samples containing *M. almatyense* (one sample) and *M. reductum* (five samples) originating from Kazakhstan and Kyrgyz Republic (detailed collection data are listed in Table 1). The samples were examined according to the protocol described by Stec et al. (2015). The extracted specimens were afterwards split into four analyses: (i) imaging and morphometry in phase-contrast light microscopy (PCM), (ii) DNA extraction and sequencing, (iii) imaging in scanning electron microscopy (SEM) and (iv) developmental variability analysis (Morek et al. 2016a). The exact numbers of specimens per population utilised for each analysis are provided in Table 1.

In addition to the new populations, paratypes of both species were examined: a single specimen of *M. al-*

*matyense* (slide No. 199) and five specimens of *M. reductum* (slide No. 192). The slides were loaned from the Zoological Institute of the Russian Academy of Sciences, St. Petersburg, Russia.

## Microscopy, imaging and morphometry

The specimens were mounted on permanent microscope slides according to the method by Morek et al. (2016b). The measurements of buccal tube follow Michalczyk et al. (2012a, b), whereas the remaining traits were measured following Tumanov (2006). The branch height ratio is a ratio of the secondary to the primary branch height and it is expressed as a percentage. The *pt* is a ratio of a given structure to the length of the buccal tube (Pilato 1981), expressed as a percentage and, in the text and tables, is given in *italics*. The number of measured specimens follows the recommendations by Stec et al. (2016). The morphometric data were handled using the Apochela spreadsheet ver. 1.3., available from Tardigrada Register, www.tardigrada.net (Michalczyk and Kaczmarek 2013). The measurements and photographs were taken with an Olympus BX53 PCM associated with an Olympus DP74 digital camera. For deep focus structures that could not be focused in a single photo, a series of up to 24 photos were taken and then merged into one focused image using Corel Photo-Paint X8. Specimens were processed for SEM imaging according to the protocol by Stec et al. (2015) and examined under high vacuum with Versa 3D DualBeam SEM at the ATOMIN facility of the Jagiellonian University.

## Developmental variability analysis

Cultures were established from live specimens and viable eggs deposited in exuviae, which were incubated at standard rearing conditions described by Kosztyła et al. (2016) with rotifers *Lecane inermis* Bryce, 1892, as a food source. In order to test for the potential presence of developmental variability, hatching was applied because developmental tracking (Morek et al. 2016a) failed (hatchlings died before reaching the juvenile stage). As ontogenetic variability in CC in both analysed species was detected, we further applied the analytical method described by Surmacz et al. (2020) to assess whether our morphometric dataset encompassed juveniles in addition to hatchlings and adults and to determine whether the species exhibit early or late CC change.

Moreover, the analytical method by Surmacz et al. (2020) was also applied to data available for *M. berladnicorum* Ciobanu et al., 2014 from the Tardigrada Register and an additional, topotypic hatchling (exhibiting the [2-2]-[2-2] CC), to test whether the species exhibits the early or late change. The data unequivocally indicated the early positive shift to [2-3]-[2-2] CC (see also Suppl. material 1).

**Table 1.** The collection details of populations analysed in this study. Analysis types: LCM – morphometry and general morphology in PCM; DNA – DNA extraction and sequencing; SEM – imaging in SEM; DEV – developmental analysis (hatching). The "?" indicates the lacking sequence.

| Sample code | Locality | Coordinates Altitude | Sample type | Specimens analysed | | | | GenBank accession numbers |
|---|---|---|---|---|---|---|---|---|
| | | | | LCM | DNA | SEM | DEV | |
| KZ.003 | Kazakhstan, Ile-Alatau | 43°1'54.6"N, 76°36'54.36"E, 1866 m asl | lichen | 3 | 4 | 10 | 2 | 18S rRNA: MT509118; 28S rRNA: MT509119; ITS-2: MT509111; COI: MT511064 |
| KG.012 | Kyrgyz Republic, Tashkömür | 41°22'22.2"N, 72°14'43.02"E, 726 m asl | moss +lichen | 5 | 4 | 5 | 2 | 18S rRNA: MT509115; 28S rRNA: MT509120; ITS-2: MT509112; COI: MT511060, MT511061 |
| KG.013 | Kyrgyz Republic, Tashkömür | 41°22'22.5"N, 72°14'46.62"E, 762 m asl | moss +lichen | 24 | 4 | 5 | 0 | 18S rRNA: MT509115; 28S rRNA: ?; ITS-2: MT509112; COI: MT511060 |
| KG.014 | Kyrgyz Republic, Tashkömür | 41°22'23.22"N, 72°14'48.3"E, 784 m asl | moss +lichen | 4 | 4 | 0 | 0 | 18S rRNA: MT509116; 28S rRNA: MT509121; ITS-2: MT509113; COI: MT511062 |
| KG.142 | Kyrgyz Republic, Toluk | 41°55'7.86"N, 73°37'49.32"E, 1520 m asl | lichen | 18 | 4 | 10 | 0 | 18S rRNA: MT509117; 28S rRNA: MT509122; ITS-2: MT509114; COI: MT511063 |
| KG.147 | Kyrgyz Republic, Toluk | 41°55'6.42"N, 73°37'52.74"E, 1522 m asl | moss +lichen | 4 | 1 | 0 | 0 | 18S rRNA: MT509115; 28S rRNA: MT509123; ITS-2: MT509114; COI: MT511063 |

## Genotyping

Genomic DNA was extracted from four individuals from each of the six analysed populations (except for a single population of *M. reductum* where only one specimen was sequenced). The extraction method follows *Chelex*® 100 resin (Bio-Rad) protocol by Casquet et al. (2012), with modifications by Stec et al. (2015). Prior to extraction, the specimens were mounted on temporary water slides to determine their CC. Whenever possible, voucher specimens were obtained from the extraction vial (in total 13 vouchers out of 21 extractions). Four genetic markers were sequenced, three nuclear: the small ribosomal subunit (18S rRNA), large ribosomal subunit (28S rRNA), Internal Transcribed Spacer 2 (ITS-2); and one mitochondrial, Cytochrome Oxidase C subunit I (COI). The PCR protocols follow Stec et al. (2015), primers and PCR programmes with relevant references are listed in Table 2. The chromatograms were manually checked using BioEdit ver. 7.2.5 (Hall 1999). As the COI is a protein coding gene, the obtained fragments were translated into amino acids using MEGA 7 (Kumar et al. 2016) to test against pseudogenes. All sequences are deposited in GenBank (the accession numbers are listed in Table 1).

## Phylogenetic analysis

To uncover the phylogenetic relationships of the two analysed species, the recent dataset by Morek and Michalczyk (2020) comprising 34 *Milnesium* populations was utilised. To this dataset, we added the 23 new sequences representing the six populations and four DNA fragments (with only a single 28S rRNA sequence for *M. reductum*, population KG.013, lacking). First, the nucleotide sequence of each marker was aligned using MAFFT version 7 (Katoh et al. 2002; Katoh and Toh 2008), with the default settings used for ITS-2 and COI, whereas for 18S rRNA and 28S rRNA, the Q-INS-I strategy was applied. As the outgroup, the following taxa were utilised: *Mesobiotus philippinicus* Mapalo et al., 2016 (18S rRNA: KX129793, 28S rRNA: KX129794, ITS-2: KX129795 and COI: KX129796; Mapalo et al. 2016), *Macrobiotus hannae* Nowak & Stec, 2018 (18S rRNA: MH063922, 28S rRNA: MH063924, ITS-2: MH063923 and COI: MH057764; Nowak and Stec 2018) and *Paramacrobiotus lachowskae* Stec et al., 2018 (18S rRNA: MF568532, 28S rRNA: MF568533, ITS-2: MF568535 and COI: MF568534; Stec et al. 2018a). In next step, the obtained alignments were visually checked in BioEdit and trimmed to 1047 (18S rRNA), 865 (28S rRNA), 648 bp (ITS-2) and 580 bp (COI). Afterwards, the four obtained alignments were concatenated in SequenceMatrix (Vaidya et al. 2011). We used the Bayesian Information Criterion in PartitionFinder version 2.1.1 (Lanfear et al. 2016) in order to find the most suitable substitution model for posterior phylogenetic analysis. As the COI is a protein coding fragment, before partitioning, the alignment was always divided into three data blocks constituting three separated codon positions. The analysis was run to test for all possible models implemented in the programme (for further, Bayesian Inference, BI). The best fit-models for six partitions in BI were: GTR+I+G for 18S rRNA, 28S rRNA, the second and the third codon positions in COI, whereas the GTR+G was indicated for ITS-2 and the first codon position in COI.

BI marginal posterior probabilities were calculated using MrBayes v3.2 (Ronquist and Huelsenbeck 2003). Ran-

**Table 2.** PCR protocols and primers references for specific protocols for amplification of the four DNA fragments sequenced in the study.

| DNA fragment | Primer name | Primer direction | Primer sequence (5'-3') | Primer source | PCR programme |
|---|---|---|---|---|---|
| **18S rRNA** | 18S_Tar_Ff1 | forward | AGGCGAAACCGCGAATGGCTC | Stec et al. (2017) | Zeller (2010) |
| | 18S_Tar_Rr1 | reverse | GCCGCAGGCTCCACTCCTGG | | |
| **28S rRNA** | 28S_Eutar_F | forward | ACCCGCTGAACTTAAGCATAT | Gąsiorek et al. (2018) | Mironov et al. (2012) |
| | 28SR0990 | reverse | CCTTGGTCCGTGTTTCAAGAC | Mironov et al. (2012) | |
| **ITS-2** | ITS2_Eutar_Ff | forward | GCATCGATGAAGAACGCAGC | Stec et al. (2018b) | Stec et al. (2018b) |
| | ITS2_Eutar_Rr | reverse | TCCTCCGCTTATTGATATGC | | |
| **COI** | COI_Mil.tar_Ff | forward | TATTTTATTTTTGGTATTTGATGTGC | Morek et al. (2019b) | Morek et al. (2019b) |
| | COI_Mil.tar_Rr | reverse | CCTCCCCCTGCAGGATC | | |
| | jjLCO1490 | forward | TITCIACIAAYCAYAARGAYATTGG | Astrin and Stüben (2008) | Michalczyk et al. (2012ab) |
| | jjHCO2198 | reverse | TAIACYTCIGGRTGICCRAARAAYCA | | |

dom starting trees were utilised and the analysis was run for ten million generations, sampling the Markov chain every 1000 generations. An average standard deviation of split frequencies of < 0.01 was used as an indicator that the two independent analyses had converged. We used Tracer v1.3 (Rambaut et al. 2014) to ensure Markov chains had reached stationarity and to determine the correct "burn-in" for the analysis (the first 10% of generations). A consensus tree was obtained after summarising the resulting topologies and discarding the "burn-in". In the BI consensus tree, clades recovered with posterior probability (PP) between 0.95 and 1.00 were considered well supported, those with PP between 0.90 and 0.94 were considered moderately supported and those with lower PP were considered unsupported. The consensus tree was visualised in FigTree v.1.4.3, available from http://tree.bio.ed.ac.uk/software/figtree.

As the dataset analysed herein is only slightly larger than the dataset by Morek and Michalczyk (2020), we did not perform the Maximum Likelihood analysis, as previously it resulted in weakly-supported nodes.

# Results

## Genetic diversity of analysed populations

*Milnesium almatyense* was represented by single haplotype in each gene, whereas *M. reductum* exhibited three 18S rRNA haplotypes, four 28S rRNA haplotypes, three ITS-2 haplotypes and four haplotypes of COI. The maximum genetic distance between the analysed populations of *M. reductum* was as follows: 0.2% in 18S rRNA, 0.5% in 28S rRNA, 1.3% in ITS-2 and 2.9% in COI, thus there was very little structuring within the *M. reductum* clade. The summary of haplotypes and the matrices of genetic distances between the populations are available in Suppl. materials 2.

## Novel morphological traits

Thanks to the observations in high quality PCM and SEM, as well as morphometric measurements of multiple specimens, including sexually-immature instars (the analysis with the algorithm developed by Surmacz et al. 2020, confirmed the presence of the first three life stag-

es), we were able to identify novel traits and update differential diagnoses for both species.

Specifically, for *M. almatyense* (Fig. 2A):

1. Morphometric data missing in the original description, such as the dimensions of peribuccal and lateral papillae, anterior and posterior widths of buccal tube, II internal, I–III external and anterior claws lengths, are provided in Table 3. Morphometric ranges have expanded in the majority of traits due to the increased sample size (six in the original description and 13 herein), but mostly because of the inclusion of immature life stages, which were not present in the original description. The only discrepancy in the measurements was the standard buccal tube width both in absolute and relative dimensions (14.1–16.3 μm and *36.5–44.0* in the original description vs. 6.5–13.1 μm and *26.2–33.1* herein). The gap in absolute dimensions can be explained by the corresponding gap in body lengths between the type series and the new population analysed herein: 672–798 μm vs. 311–665 μm, respectively (Tumanov 2006 measured only larger specimens, hence the skewed body size in the original description). The gap in relative values is harder to explain, but (i) the *pt* index does not remove the allometric effects entirely (Bartels et al. 2011) and (ii) buccal tube width is susceptible to deformation under cover-glass pressure and even minor changes in pressure may considerably affect *pt* values (Morek et al. 2016b). Importantly, the susceptibility to deformation increases with the size of the buccal tube (Morek et al. 2016b), thus, given that larger specimens were present in the type series than in the new population, any differences in cover-slip pressure would magnify the effect, resulting in a discrepancy in buccal tube width. Thus, we consider the gaps in buccal tube width between the type series and the new population analysed herein as an artefact caused by differences in body size, possibly magnified by differences in cover-slip pressure.

2. The analysis of ontogenetic variability in CC showed that hatchlings (Fig. 1A) exhibit a [2-2]-[2-2] CC (Fig. 1B), whereas juveniles and adults have
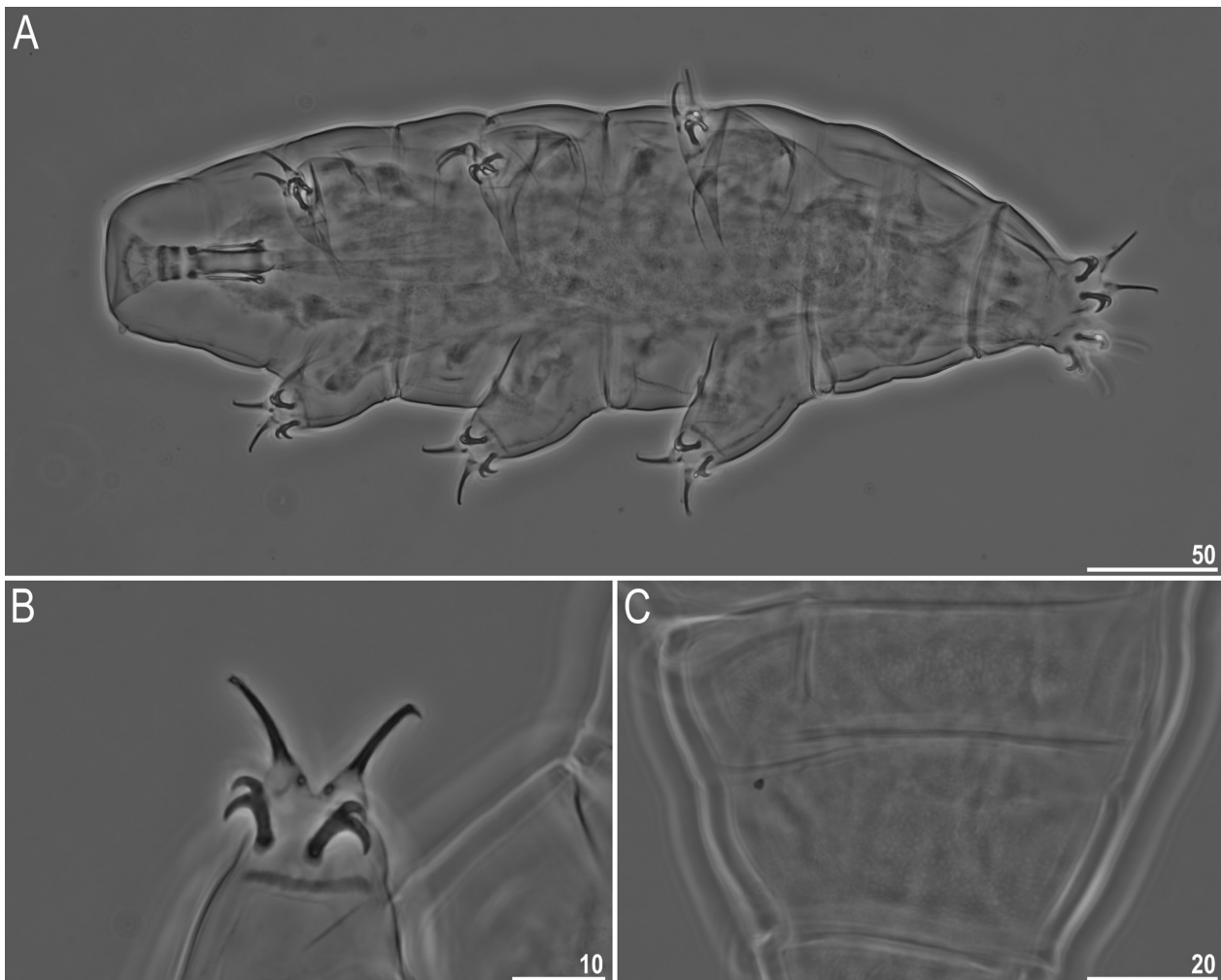
**Figure 1.** The morphology of *Milnesium almatyense* Tumanov, 2006 hatchlings, PCM. **A** Habitus; **B** Claws II, with the [2-2] CC; **C** Dorsal cuticle with visible sculpture in form of reticulation. All the scale bars are given in µm.

a [2-3]-[2-2] CC (Fig. 2D), thus the species undergoes the early positive anterior CC change (see also Suppl. material 3).

3. As there are recognised species characterised exclusively by a [2-2]-[2-2] CC, they need to be compared with hatchlings of *M. almatyense* to ensure they, indeed, represent different species. Specifically, *M. katarzynae* Kaczmarek et al., 2004 differs from *M. almatyense* by more posteriorly-inserted stylet supports (*73.3–78.3* in *M. katarzynae* vs. *70.2–70.7* in hatchlings of *M. almatyense*), whereas *M. kogui* Londoño et al., 2015 differs from *M. almatyense* by relatively shorter primary branches IV (*37.9–40.4* in *M. kogui* vs. *52.0–65.9* in hatchlings of *M. almatyense*).

4. Observation of the mouth opening in SEM confirmed that the species has six peribuccal lamellae, but it also indicated that the lamellae are of unequal size, i.e. the pair of dorsal and ventral lamellae are larger than the two lateral lamellae, i.e. the configuration is 4+2 (Fig. 2C).

5. Observations under a high quality PCM and SEM indicated that *M. almatyense* has a sculptured cuticle, which is visible both, in the population analysed herein (Fig. 3A, C, E, F), as well as in the analysed paratype (Fig. 3B, D). The sculpturing has a form of delicate, irregular wrinkles, similarly to *M. berladnicorum* and *M. variefidum* (Morek et al. 2016a). Pseudopores and dorsal pseudoplates are also clearly visible in the analysed paratype (Fig. 3B) and the new population (the scheme of the pseudoplate arrangement is depicted in Fig. 2B, based on the new population). Row I is not visible, whereas for rows II and III, the determination of exact shape was impossible, due to the obscured outline of the pseudoplates (numbering according to Moreno-Talamantes et al. 2019). The cuticle in hatchlings is similar, but the dorsal sculpture is more evident and regular, forming a delicate reticulation (Fig. 1C).

Similarly, for *M. reductum* (Fig. 4A):

1. Morphometric data missing in the original description, such as the dimensions of peribuccal and lateral papillae, anterior and posterior widths of buccal tube, II internal, I–III external and anterior claws

**Table 3.** Measurements (in μm) and the *pt* values of selected morphological structures of 13 adult females of *Milnesium almatyense* Tumanov, 2006 from Kazakhstan, KZ.003, mounted in Hoyer's medium. All available specimens were measured (N – number of specimens/structures measured, RANGE refers to the smallest and the largest structure amongst all measured specimens; SD – standard deviation).

| Character | N | Range | | Mean | | SD | |
|---|---|---|---|---|---|---|---|
| | | μm | pt | μm | pt | μm | pt |
| Body length | 13 | 311–665 | 1254–1679 | 502 | 1512 | 107 | 122 |
| Peribuccal papillae length | 9 | 4.9–8.2 | 14.6–21.1 | 6.4 | 19.3 | 1.0 | 2.1 |
| Lateral papillae length | 12 | 3.6–6.0 | 12.2–15.8 | 4.8 | 14.7 | 0.9 | 1.0 |
| Buccal tube | | | | | | | |
| Length | 13 | 24.6–40.2 | – | 32.9 | – | 5.2 | – |
| Stylet support insertion point | 12 | 17.4–28.4 | 67.0–71.9 | 22.8 | 69.6 | 3.7 | 1.6 |
| Anterior width | 10 | 7.8–16.0 | 31.7–41.3 | 12.1 | 36.2 | 2.9 | 3.2 |
| Standard width | 10 | 6.5–13.1 | 26.2–33.1 | 10.0 | 29.9 | 2.2 | 2.2 |
| Posterior width | 10 | 6.6–13.7 | 26.6–35.9 | 10.0 | 30.0 | 2.4 | 2.9 |
| Standard width/length ratio | 10 | 26%–33% | – | 30% | – | 2% | – |
| Posterior/anterior width ratio | 10 | 73%–92% | – | 83% | – | 7% | – |
| Claw 1 heights | | | | | | | |
| External primary branch | 11 | 10.4–16.6 | 39.3–49.2 | 13.8 | 42.3 | 2.1 | 2.6 |
| External base + secondary branch | 7 | 9.0–16.2 | 35.3–42.4 | 13.0 | 38.5 | 2.6 | 2.4 |
| External branches length ratio | 6 | 87%–98% | – | 93% | – | 4% | – |
| Internal primary branch | 12 | 9.7–15.6 | 35.6–48.8 | 13.1 | 40.1 | 1.8 | 3.2 |
| Internal base + secondary branch | 8 | 8.6–15.4 | 34.2–39.8 | 12.2 | 37.1 | 2.2 | 2.0 |
| Internal spur | 6 | 3.4–5.3 | 11.7–13.6 | 4.4 | 12.6 | 0.7 | 0.8 |
| Internal branches length ratio | 8 | 89%–100% | – | 94% | – | 4% | – |
| Claw 2 heights | | | | | | | |
| External primary branch | 13 | 11.3–19.3 | 42.5–56.1 | 15.4 | 47.0 | 2.4 | 3.2 |
| External base + secondary branch | 11 | 9.0–16.3 | 36.3–44.8 | 13.3 | 40.5 | 2.3 | 2.2 |
| External branches length ratio | 11 | 74%–96% | – | 86% | – | 6% | – |
| Internal primary branch | 12 | 10.6–17.5 | 41.5–50.4 | 14.8 | 44.3 | 2.1 | 2.4 |
| Internal base + secondary branch | 9 | 8.7–15.8 | 35.1–41.4 | 13.1 | 38.3 | 2.0 | 1.9 |
| Internal spur | 7 | 4.3–5.4 | 12.3–15.6 | 4.7 | 13.7 | 0.5 | 1.4 |
| Internal branches length ratio | 9 | 82%–92% | – | 88% | – | 3% | – |
| Claw 3 heights | | | | | | | |
| External primary branch | 12 | 10.9–19.6 | 44.0–56.1 | 15.8 | 48.8 | 2.4 | 3.3 |
| External base + secondary branch | 10 | 8.6–17.2 | 34.7–44.8 | 13.5 | 41.6 | 2.9 | 3.0 |
| External branches length ratio | 9 | 71%–91% | – | 85% | – | 7% | – |
| Internal primary branch | 9 | 10.8–19.3 | 43.5–48.7 | 15.4 | 46.3 | 2.8 | 1.8 |
| Internal base + secondary branch | 8 | 9.6–16.6 | 39.0–47.3 | 13.9 | 41.3 | 2.5 | 2.6 |
| Internal spur | 9 | 3.8–7.2 | 10.8–18.2 | 4.7 | 13.7 | 1.0 | 1.9 |
| Internal branches length ratio | 6 | 83%–91% | – | 87% | – | 3% | – |
| Claw 4 heights | | | | | | | |
| Anterior primary branch | 7 | 12.9–23.6 | 52.0–63.4 | 18.5 | 58.5 | 3.7 | 3.4 |
| Anterior base + secondary branch | 9 | 9.8–19.7 | 39.5–50.2 | 15.1 | 45.9 | 3.5 | 3.4 |
| Anterior branches length ratio | 6 | 68%–85% | – | 78% | – | 6% | – |
| Posterior primary branch | 9 | 13.0–23.6 | 52.0–65.9 | 19.0 | 59.6 | 3.4 | 4.8 |
| Posterior base + secondary branch | 8 | 10.1–19.7 | 40.7–52.3 | 15.4 | 47.5 | 3.1 | 3.6 |
| Posterior branches length ratio | 7 | 74%–84% | – | 80% | – | 3% | – |

lengths, are provided in Table 4. Morphometric ranges have slightly expanded in the majority of traits due to the increased sample size (six in the original description and 34 herein) and mostly because of the inclusion of immature life stages, which were not recognised in the original description.

2. The analysis of ontogenetic variability in CC showed that hatchlings exhibit a [2-2]-[2-2] CC (Fig. 5A, B), whereas juveniles and adults have a [2-3]-[3-2] CC (Fig. 5C), thus the species undergoes the early positive CC change (see also Suppl. material 4). SEM observations confirmed that the accessory points on primary branches are, indeed, lacking (Fig. 5C, D).

3. As there are described species characterised exclusively by a [2-2]-[2-2] CC, they need to be compared with hatchlings of *M. reductum*. Both *M. katarzynae* and *M. kogui* differ from *M. reductum* by having accessory points on primary branches (clearly visible in PCM).

4. SEM observations confirmed that the species has six peribuccal lamellae, but it also indicated that the lamellae are of unequal size, i.e. the pair of dorsal and ventral lamellae are larger than the two lateral lamellae, i.e. the configuration is 4+2 (Fig. 4B).

5. Observations under a high quality PCM of all new populations, as well as of the analysed paratype, revealed that this species possesses pseudopores visible in the dorsal cuticle (Fig. 4D, E). A weak outline of a single pseudoplate is also visible (Fig. 4C, E). The SEM imaging further confirmed the species has s smooth dorsal cuticle, with a barely visible pseudoplate in row VIII (Fig. 4C). As only a single pseudoplate is observable both in PCM and SEM, a scheme of pseudoplate arrangement is not provided.
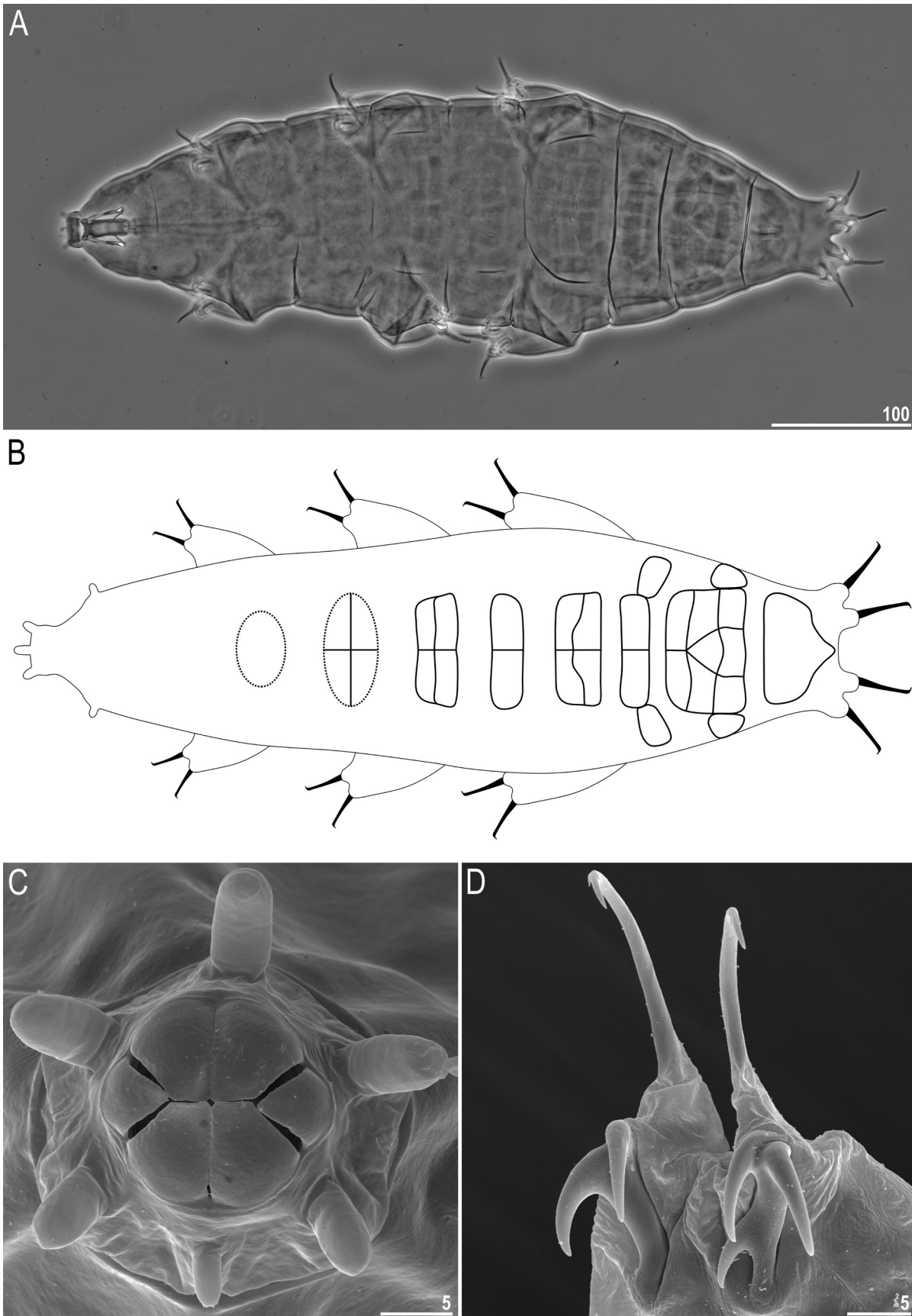
**Figure 2.** The morphology of *Milnesium almatyense* Tumanov, 2006 adults. **A** Habitus, PCM; **B** The pseudoplate arrangement based on adult specimens from population KZ.003, drawing; **C** SEM photograph of mouth opening; with six, unequal in size peribuccal lamellae, so-called 4+2 configuration; **D** SEM photograph of claws II with a [2-3] CC and visible accessory points. All the scale bars are given in μm.
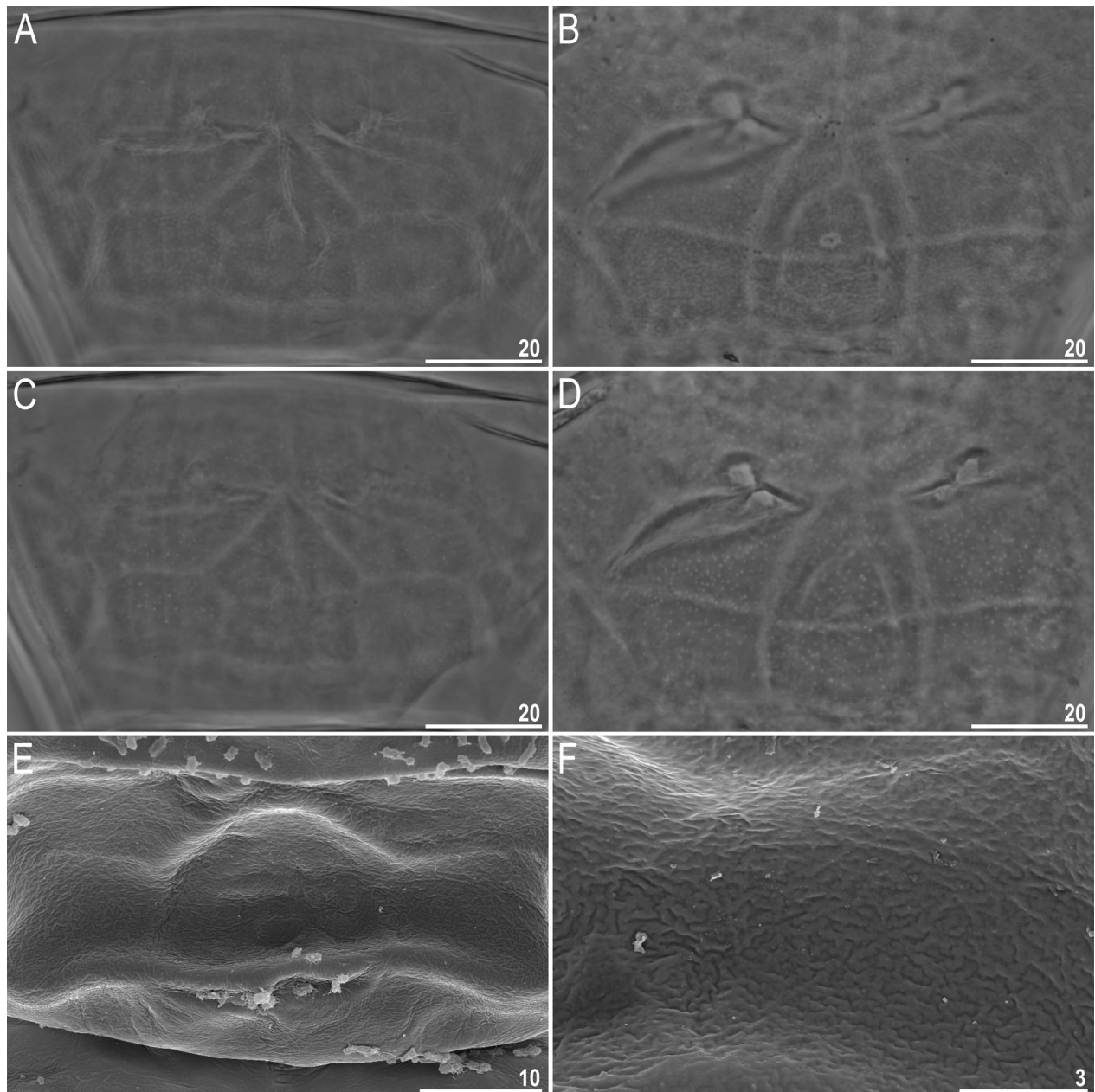
**Figure 3.** The morphology of *Milnesium almatyense* Tumanov, 2006 adults cuticle. A Sculptured dorsal cuticle, with visible pseudoplates, specimen from KZ.003 population, PCM; **B** Sculptured dorsal cuticle, with visible pseudoplates, paratype, PCM; **C** Dorsal cuticle with visible pseudopores, the same specimens on A from KZ.003 population, PCM; **D** Dorsal cuticle with visible pseudopores, paratype, PCM. **E** SEM photograph of dorsal cuticle with visible sculpture and caudal, complex pseudoplate. **F** SEM photograph of details of sculpture of the dorsal cuticle. The photographs **A** and **C**, as well as **B** and **D** depict the same specimen and paratype, respectively. All the scale bars are given in μm.

## Phylogenetic position of *M. almatyense* and *M. reductum*

Adding the two species to the dataset published by Morek and Michalczyk (2020) did not alter the overall topology of *Milnesium* phylogenetic tree (see figure 3 therein). Both species are embedded in "clade A" (*sensu* Morek and Michalczyk 2020), which is shown in Fig. 6. *M. almatyense* is recovered as a sister species to *M. berladnicorum*, both

being in a polytomy with *M. variefidum* Morek et al. 2016a and a well-supported subclade comprising *M. tardigradum* Doyère, 1840 and *M. pseudotardigradum* Surmacz et al. 2019. On the other hand, *M. reductum* is represented by five closely-related populations forming a well-supported subclade that is in a sister relationship with all remaining taxa of "clade A" in Morek and Michalczyk (2020).

In the currently available dataset, the species with the closest affinity to *M. almatyense* is *M. berladnicorum*,

**Table 4.** Joined measurements (in μm) and the *pt* values of selected morphological structures of 34 adult females of *Milnesium reductum* Tumanov, 2006 from five populations from Kyrgyz Republic, KG.012; KG.013; KG.014, KG.142 and KG.147, mounted in Hoyer's medium. Individuals were chosen to represent the entire body length range, with as equal representation of all available life stages as possible (N – number of specimens/structures measured, RANGE refers to the smallest and the largest structure amongst all measured specimens; SD – standard deviation).

| Character | N | Range | | Mean | | SD | |
|---|---|---|---|---|---|---|---|
| | | μm | *pt* | μm | *pt* | μm | *pt* |
| Body length | 31 | 363–730 | *1217–1693* | 555 | *1535* | 143 | *110* |
| Peribuccal papillae length | 30 | 3.7–8.8 | *13.3–22.1* | 6.4 | *17.8* | 1.3 | *2.1* |
| Lateral papillae length | 31 | 4.6–10.0 | *14.6–23.7* | 7.1 | *19.1* | 1.6 | *2.2* |
| Buccal tube | | | | | | | |
| Length | 34 | 25.8–43.9 | – | 36.4 | – | 5.7 | – |
| Stylet support insertion point | 34 | 18.3–29.3 | *62.9–72.9* | 24.8 | *68.4* | 3.3 | *2.5* |
| Anterior width | 33 | 7.7–16.8 | *25.8–41.3* | 11.9 | *32.2* | 2.4 | *3.6* |
| Standard width | 33 | 5.6–16.2 | *20.0–39.8* | 9.8 | *26.4* | 2.6 | *4.6* |
| Posterior width | 33 | 6.6–17.8 | *22.2–43.7* | 11.3 | *30.3* | 2.9 | *4.7* |
| Standard width/length ratio | 33 | 20%–40% | – | 26% | – | 5% | – |
| Posterior/anterior width ratio | 33 | 74%–120% | – | 94% | – | 11% | – |
| Claw 1 heights | | | | | | | |
| External primary branch | 32 | 14.9–24.0 | *48.1–60.4* | 19.5 | *54.0* | 2.5 | *3.5* |
| External base + secondary branch | 30 | 9.2–15.1 | *28.9–38.8* | 12.7 | *34.6* | 1.7 | *2.4* |
| External branches length ratio | 28 | 57%–72% | – | 64% | – | 4% | – |
| Internal primary branch | 33 | 14.2–23.4 | *45.3–57.9* | 18.6 | *51.3* | 2.6 | *3.7* |
| Internal base + secondary branch | 33 | 8.8–14.7 | *24.4–37.4* | 12.2 | *33.6* | 1.7 | *3.2* |
| Internal spur | 26 | 4.6–8.1 | *13.1–20.7* | 6.2 | *16.4* | 0.8 | *2.0* |
| Internal branches length ratio | 32 | 53%–75% | – | 66% | – | 5% | – |
| Claw 2 heights | | | | | | | |
| External primary branch | 33 | 16.8–26.8 | *49.5–65.8* | 21.7 | *59.2* | 2.9 | *3.7* |
| External base + secondary branch | 30 | 9.8–16.0 | *33.0–40.4* | 13.1 | *36.7* | 2.0 | *1.8* |
| External branches length ratio | 29 | 56%–70% | – | 62% | – | 3% | – |
| Internal primary branch | 33 | 15.5–26.4 | *48.8–64.9* | 20.7 | *57.2* | 3.1 | *3.8* |
| Internal base + secondary branch | 30 | 8.3–17.9 | *31.7–50.7* | 13.0 | *35.8* | 2.1 | *3.5* |
| Internal spur | 25 | 5.0–8.8 | *14.8–21.3* | 7.0 | *18.3* | 0.9 | *2.1* |
| Internal branches length ratio | 29 | 50%–87% | – | 63% | – | 6% | – |
| Claw 3 heights | | | | | | | |
| External primary branch | 33 | 16.0–26.9 | *49.8–70.1* | 22.0 | *60.5* | 3.1 | *4.7* |
| External base + secondary branch | 31 | 9.3–16.2 | *32.8–42.0* | 13.5 | *36.9* | 2.0 | *2.3* |
| External branches length ratio | 30 | 53%–67% | – | 61% | – | 4% | – |
| Internal primary branch | 31 | 14.2–25.9 | *48.6–64.5* | 20.9 | *58.3* | 3.2 | *4.4* |
| Internal base + secondary branch | 28 | 9.3–16.0 | *31.7–41.2* | 13.1 | *35.8* | 2.1 | *2.3* |
| Internal spur | 26 | 5.3–9.5 | *15.0–23.3* | 7.1 | *18.6* | 1.1 | *2.1* |
| Internal branches length ratio | 26 | 53%–71% | – | 62% | – | 5% | – |
| Claw 4 heights | | | | | | | |
| Anterior primary branch | 34 | 17.4–31.3 | *59.6–80.9* | 25.7 | *70.8* | 3.9 | *4.7* |
| Anterior base + secondary branch | 32 | 9.9–20.5 | *31.3–50.4* | 14.4 | *39.6* | 2.6 | *3.3* |
| Anterior spur | 26 | 5.1–8.5 | *14.6–25.3* | 6.8 | *18.0* | 1.1 | *2.6* |
| Anterior branches length ratio | 32 | 45%–65% | – | 56% | – | 5% | – |
| Posterior primary branch | 33 | 18.4–31.5 | *61.2–82.7* | 26.2 | *72.2* | 3.8 | *5.1* |
| Posterior base + secondary branch | 33 | 9.4–19.2 | *36.4–48.8* | 15.2 | *41.7* | 2.8 | *3.2* |
| Posterior branches length ratio | 32 | 50%–65% | – | 58% | – | 4% | – |

thus we compared the genetic distances between the two species, which are as follows: 0.2% in 18S rRNA, 0.9% in 28S rRNA, 4.0% in ITS-2 and 6.9% in COI. *M. reductum* is indicated as the sister species for the entire clade (genetic distances between *M. reductum* and the remaining species of clade A are as follows: 0.5–2.4% in 18S rRNA, 3.4–5.7% in 28S rRNA, 10.2–16.3% in ITS-2 and 13.8–16.3% in COI).

Considering the similarity and problematic taxonomy of *M. tardigradum* and *M. pseudotardigradum*, as well as of *M. almatyense*, *M. berladnicorum* and *M. variefidum*, we introduce names for these two species clusters: the *tardigradum* complex and the *almatyense* complex, respectively (Fig. 6). The names are derived from the first species described within respective complexes.

## Discussion

New observations under a high class PCM and SEM, as well as ontogenetic variability analysis, allowed for a substantial amendment of the original descriptions of *M. almatyense* and *M. reductum*. Furthermore, sequencing of the four standard DNA barcodes delivered a new line of evidence supporting the erection of the two species and allowed an inference of their phylogenetic positions. DNA barcodes also provide an important and useful tool for identification of both species. Currently, integrative data are available only for 14 of 41 formally-described *Milnesium* species (34%; Michalczyk et al. 2012a, b; Morek et al. 2016a; Jackson and Meyer 2019; Kaczmarek et al. 2019; Morek et al. 2019a; Morek et
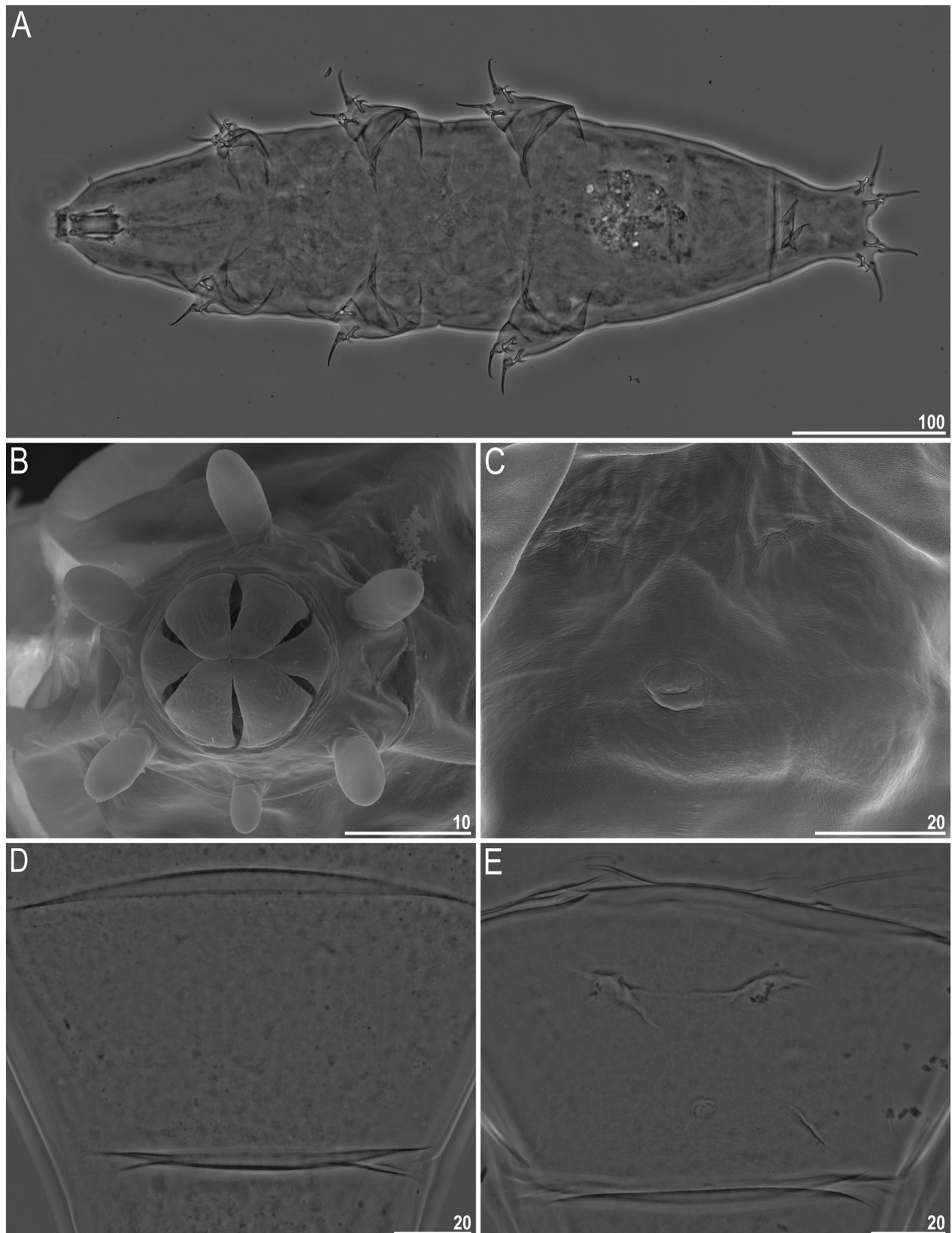
**Figure 4.** The morphology of *Milnesium reductum* Tumanov, 2006 **A** Habitus of adult female, PCM; **B** SEM photograph of mouth opening; with six, unequal in size peribuccal lamellae, so-called 4+2 configuration; **C** SEM photograph of smooth dorsal cuticle with visible single, complex pseudoplate; **D** smooth dorsal cuticle, with visible single pseudoplate and faint pseudopores, specimen from KG.013 population, PCM; **E** smooth dorsal cuticle, with visible single pseudoplate and faint pseudopores, paratype, PCM. All the scale bars are given in μm.
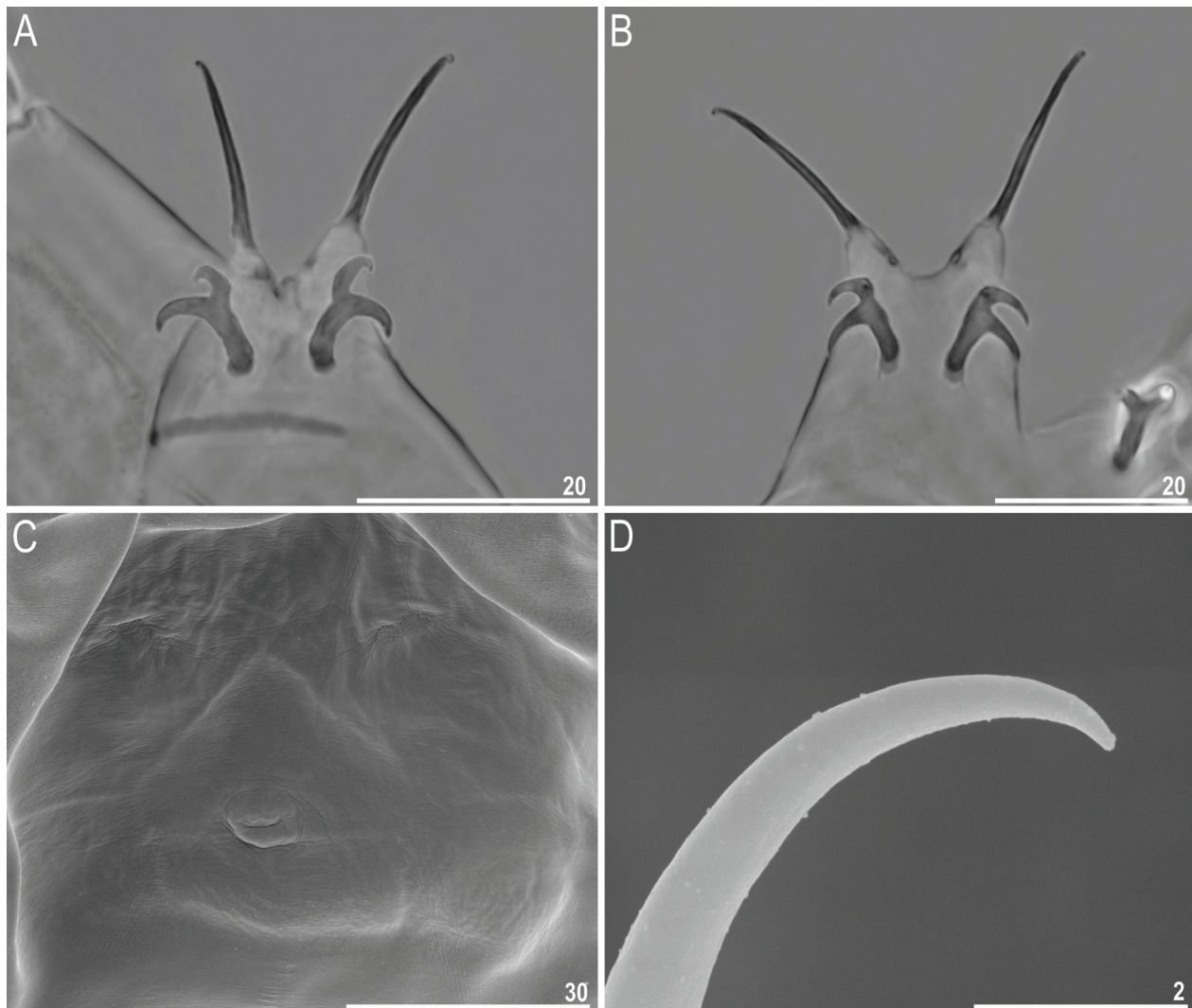
**Figure 5.** The morphology of claws of *Milnesium reductum* Tumanov, 2006 **A** Photograph of hatchlings claws III with a [2-2] CC, PCM; **B** Photograph of hatchlings claws IV with a [2-2] CC, PCM; **C** SEM photograph of claws II with a [2-3] CC lacking accessory points; **D** SEM photograph of tip of primary branch of claws lacking accessory points. All the scale bars are given in µm.

al. 2019b; Surmacz et al. 2019; Morek et al. in press; present contribution), which is a worryingly low percentage, considering the challenging taxonomy of this genus reflected by the low number of useful phenotypic traits for species differentiation and the widespread developmental variability. Moreover, within the 14 species for which integrative data are available, only in 10 species has the ontogenetic variability been analysed. This shows how much there is still to be done to stabilise *Milnesium* taxonomy, both in terms of re-descriptions and encouraging taxonomists to publish descriptions supported by ontogenetic variability and genetic analyses. Especially, that recent studies revealed a considerable undescribed species diversity within the genus (Morek and Michalczyk 2020) and demonstrated evidence for pseudocryptic *Milnesium* species (Morek et al. 2019b; Surmacz et al. 2019), the identification of which would not have been possible with the sole use of classical tools.

Although the number of species that were tested against developmental variability in CC is not too high (20 species, including the undescribed species that were analysed by Morek and Michalczyk 2020), some patterns seem to emerge. Specifically, amongst the 10 tested species with adult [3-3]-[3-3] CC, ontogenetic variability was observed only in a single species (an undescribed *Milnesium* sp. nov. 10 PH.014 in Morek and Michalczyk 2020). In contrast, all 10 tested species with adult CC different from [3-3]-[3-3], exhibited developmental variability in CC. Moreover, in the majority of cases (7 of 10 species; 70%) an increase in the number of secondary claw branches is observed (i.e. positive CC change). Importantly, in the vast majority of cases (9 of 10 species; 90%), the shift takes place between hatchlings and juveniles (i.e. early CC change). Given that hatchlings are most likely to be missing in the type series, taxonomists should be especially cautious when describing and analysing taxa in which adults exhibit the CC other than [3-3]-[3-3].
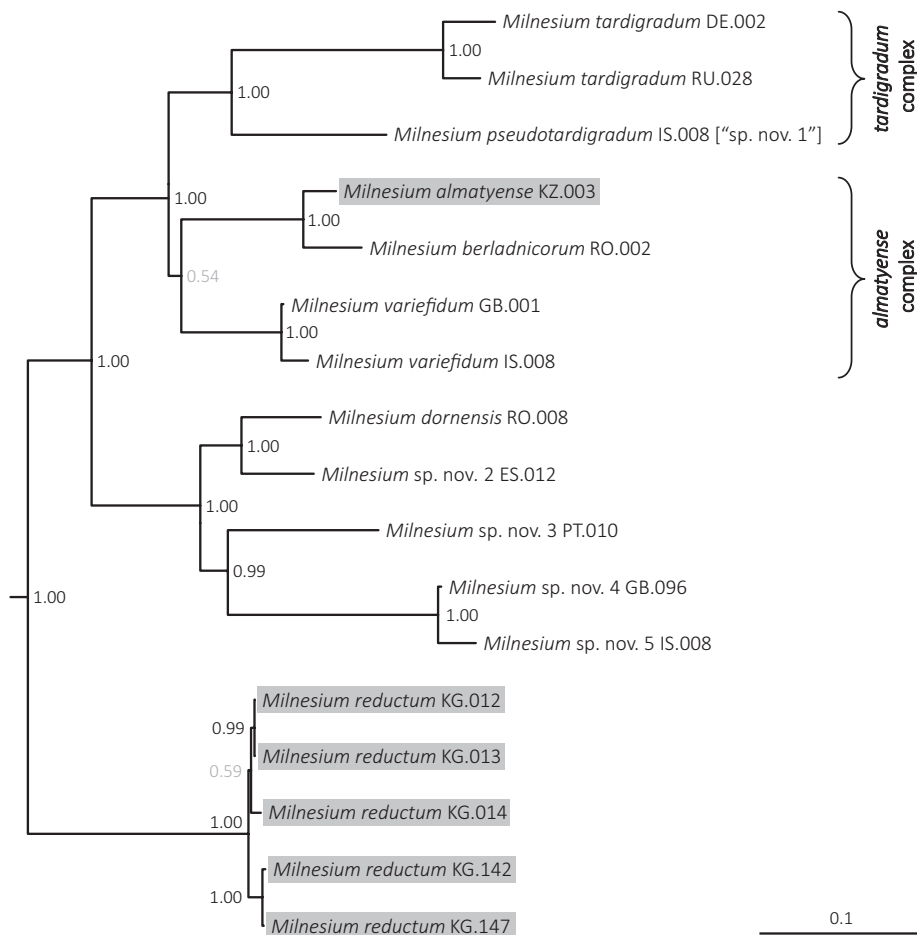
**Figure 6.** Fragment of the Bayesian phylogenetic tree ("clade A"), based on the analysis of concatenated 18S rRNA + 28S rRNA + ITS-2 + COI nucleotide sequences, obtained by Morek and Michalczyk (2020) with an addition of six new populations, showing the positions of the two *Milnesium* species analysed in this contribution (shaded in grey): *M. almatyense* Tumanov, 2006 and *M. reductum* Tumanov, 2006. The numbers at nodes represent Posterior Probability (PP) supports, with the values in grey font indicating poor support (conventionally recognised as polytomy). The scale bar shows the number of substitutions per site. For the remaining parts of the tree, please see Morek and Michalczyk (2020).

In contrast to the original description of *M. almatyense*, our analysis of the type and new material showed that the dorsal cuticle is not smooth, but covered with fine sculpturing and pseudoplates. These characteristics were missed due to the insufficient quality of the light microscope used by Tumanov (2006) and because such traits were not recognised at the time. This amendment, along with the exact same pattern of ontogenetic CC change (i.e. early positive) makes *M. almatyense* extremely similar to *M. berladnicorum*. Specifically, in the original differential diagnosis of *M. berladnicorum* (Ciobanu et al. 2014), the species was discriminated from *M. almatyense* by the sculptured cuticle and ontogenetic variability in CC was not known to occur in either species. Moreover, measurements of all morphometric traits presented herein (Table 3) and in the original description (Table 3 in Tumanov 2006) overlap with ranges for *M. berladnicorum*. Another trait used by Ciobanu et al. (2014) to differentiate *M. berladnicorum* from *M. almatyense* was the lack of eyes in *M. almatyense*.

However, the absence of eyes was observed by Tumanov (2006) in specimens fixed on microscope slides, thus it is not known whether the eyes were absent or they were present in living animals, but they dissolved in acetic acid and Faure medium (D. Tumanov, pers. inf.). Importantly, the eyes were present in all living individuals in the *M. almatyense* population analysed herein and dissolved in Hoyer's medium in hatchlings. Thus, it could be assumed that *M. almatyense* exhibits eyes as *M. berladnicorum* does, making this trait invalid in the differentiation of these two species. We have, however, found a single morphological trait that could potentially differentiate *M. almatyense* and *M. berladnicorum*: pseudoplate arrangement, specifically in *M. almatyense* pseudoplate IV is singular (Fig. 2B), but it is double in *M. berladnicorum* (fig. 6A in Morek et al. 2016a). However, the taxonomic value of dorsal pseudoplates in *Milnesium* has been recently questioned by Moreno-Talamantes et al. (2019). Thus, further studies on this trait are needed to validate its value in species differentiation.

Moreover, the new genetic data, presented herein, show that *M. almatyense* and *M. berladnicorum* are a pair of a very closely-related species (Fig. 6), with genetic distances in the analysed variable markers between the two species being moderate in both ITS-2 (4.0%) and COI (6.9%). Considering that there are *Milnesium* species with high intraspecific genetic distances (e.g. *M. tardigradum* with p-distances up to 4.0% in ITS-2 and 11.4% in COI, Morek et al. 2019b or *M. eurystomum* Maucci, 1991 with respective maximum distances of 1.7% and 8.9%, Morek et al. in press), it is not clear whether *M. almatyense* and *M. berladnicorum* are a single or distinct species. Thus, a more detailed analysis, for example, with the use of new genetic markers, is needed to verify whether *M. berladnicorum* is a good species or a junior synonym of *M. almatyense*. If the taxonomic status of *M. berladnicorum* is supported, then this pair of species should be considered pseudocryptic, as the phenotypic differences are difficult to spot and are not straightforward. In other words, a confident identification of these species may require DNA barcoding.

The recent phylogenetic analysis of the genus *Milnesium* suggested that species generally cluster by geography (Morek and Michalczyk 2020). Thus, as both *M. almatyense* and *M. reductum* originate from the Palearctic realm (*sensu* Holt et al., 2013), we expected them to be placed either in clade A or clade B shown by Morek and Michalczyk (2020) and the current analysis confirmed this prediction by demonstrating that both species represent clade A (Fig. 6). Therefore, the correlation between molecular phylogeny and geographic origin of populations is maintained and strengthened. *M. reductum* is so far the only species characterised by the lack of accessory points, for which its phylogenetic position is known. Therefore, it is difficult to speculate, whether this trait was lost only once in *Milnesium* or this is yet another example of convergent evolution (as has been shown for many other traits, such as cuticular sculpturing, claw or lamellae configuration; Morek and Michalczyk 2020). However, given that generally *Milnesium* species seem to exhibit limited geographic ranges and since the other four known species that lack the accessory points originate from different zoogeographic realms, i.e. India (*M. longiungue* Tumanov, 2006) and USA (*M. alabamae* Wallendorf & Miller, 2009; *M. swansoni* Young, Chappell, Miller & Lowman, 2016 and *M. zsalakoae* Meyer & Hinton, 2010), it would not be surprising if this trait was lost independently in different lineages.

# Acknowledgements

# References

Astrin JJ, Stüben PE (2008) Phylogeny in cryptic weevils: molecules, morphology and new genera of western Palaearctic Cryptorhynchinae (Coleoptera: Curculionidae). Invertebrate Systematics 22(5): 503–522. https://doi.org/10.1071/IS07057

Bartels PJ, Nelson DR, Exline RP (2011) Allometry and the removal of body size effects in the morphometric analysis of tardigrades. Journal of Zoological Systematics and Evolutionary Research 49: 17–25. https://doi.org/10.1111/j.1439-0469.2010.00593.x

Bryce D (1892) On the Macrotrachelous Callidinae. Journal of the Quekett Microscopical Club 2: 15–23. https://doi.org/10.5962/bhl.part.18580

Casquet J, Thebaud C, Gillespie RG (2012) Chelex without boiling, a rapid and easy technique to obtain stable amplifiable DNA from small amounts of ethanol-stored spiders. Molecular Ecology Resources 12: 136–141. https://doi.org/10.1111/j.1755-0998.2011.03073.x

Ciobanu DA, Zawierucha K, Moglan I, Kaczmarek Ł (2014) *Milnesium berladnicorum* sp. n. (Eutardigrada, Apochela, Milnesiidae), a new species of water bear from Romania ZooKeys 429: 1–11. https://doi.org/10.3897/zookeys.429.7755

Coughlan K, Michalczyk Ł, Stec D (2019) *Macrobiotus caelestis* sp. nov., a new tardigrade species (Macrobiotidae: *hufelandi* group) from the Tien Shan mountains (Kyrgyzstan). Annales Zoologici 69(3): 499–513. https://doi.org/10.3161/00034541ANZ2019.69.3.002

Degma P, Bertolani R, Guidetti R (2009–2019) Actual checklist of Tardigrada species. Accessed date [01.03.2020]

Doyère ML (1840) Memorie sur les Tardigrades. Annales des Sciences Naturelles. Zoologie 14: 269–362.

Gąsiorek P, Stec D, Morek W, Michalczyk Ł (2018) An integrative redescription of *Hypsibius dujardini* (Doyère, 1840), the nominal taxon for Hypsibioidea (Tardigrada: Eutardigrada). Zootaxa 4415: 45–75. https://doi.org/10.11646/zootaxa.4415.1.2

Hall TA (1999) BioEdit: a user-friendly biological sequence alignment editor and analysis program for Windows 95/98/NT. Nucleic Acids Symposium Series 41: 95–98.

Holt BG, Lessard JP, Borregaard MK, Fritz SA, Araújo MB, Dimitrov D, Fabre PH, Graham CH, Graves GR, Jønsson KA, Nogués-Bravo D, Wang Z, Whittaker RJ, Fjeldså J, Rahbek C (2013) An Update of Wallace's Zoogeographic Regions of the World. Science 339 (6115): 74–78. https://doi.org/10.1126/science.1228282

Jackson KJA, Meyer HA (2019) Morphological and genetic analysis of *Milnesium* cf. *granulatum* (Tardigrada: Milnesiidae) from Northeastern North America. Zootaxa 4604(3): 497–510. https://doi.org/10.11646/zootaxa.4604.3.6

Kaczmarek Ł, Michalczyk Ł, Beasley CW (2004) *Milnesium katarzynae*, a new species of Eutardigrade (Milnesiidae) from China. Zootaxa 743: 1–5. https://doi.org/10.11646/zootaxa.743.1.1

Kaczmarek Ł, Zawierucha K, Buda J, Stec D, Gawlak M, Michalczyk Ł, Roszkowska M (2018) An integrative redescription of the nominal taxon for the *Mesobiotus harmsworthi* group (Tardigrada: Macrobiotidae) leads to descriptions of two new *Mesobiotus* species from Arctic. PLoS ONE 13(10): pe0204756. https://doi.org/10.1371/journal.pone.0204756

Kaczmarek Ł, Grobys D, Kulpa A, Bartylak T, Kmita H, Kepel M, Kepel A, Roszkowska M (2019) Two new species of the genus *Milnesium* Doyère, 1840 (Tardigrada, Apochela, Milnesiidae) from Madagascar. ZooKeys 884: 1–22. https://doi.org/10.3897/zookeys.884.29469

Katoh K, Misawa K, Kuma K, Miyata T (2002) MAFFT: A novel method for rapid multiple sequence alignment based on fast Fourier transform. Nucleic Acids Resources 30: 3059–3066. https://doi.org/10.1093/nar/gkf436

Katoh K, Toh H (2008) Recent developments in the MAFFT multiple sequence alignment program. Brief Bioinformatics 9: 286–298. https://doi.org/10.1093/bib/bbn013

Kosztyła P, Stec D, Morek W, Gąsiorek P, Zawierucha K, Michno K, Ufir K, Małek D, Hlebowicz K, Laska A, Dudziak M, Frohme M, Prokop ZM, Kaczmarek Ł, Michalczyk Ł (2016) Experimental taxonomy confirms the environmental stability of morphometric traits in a taxonomically challenging group of microinvertebrates. Zoological Journal of the Linnean Society 178: 765–775. https://doi.org/10.1111/zoj.12409

Kumar S, Stecher G, Tamura K (2016) MEGA7: Molecular Evolutionary Genetics Analysis version 7.0 for bigger datasets. Molecular Biology and Evolution 33: 1870–1874. https://doi.org/10.1093/molbev/msw054

Lanfear R, Hua X, Warren DL (2016) Estimating the effective sample size of tree topologies from Bayesian phylogenetic analyses. Genome Biology and Evolution 8: 2319–2332. https://doi.org/10.1093/gbe/evw171

Londoño R, Daza A, Caicedo M, Quiroga S, Kaczmarek Ł (2015) The genus *Milnesium* (Eutardigrada: Milnesiidae) in the Sierra Nevada de Santa Marta (Colombia), with the description of *Milnesium kogui* sp. nov. Zootaxa 3955(4): 561–568. https://doi.org/10.11646/zootaxa.3955.4.7

Mapalo MA, Stec D, Mirano-Bascos D (2016) *Mesobiotus philippinicus* sp. nov., the first limnoterrestrial tardigrade from the Philippines. Zootaxa 4126(3): 411–426. https://doi.org/10.11646/zootaxa.4126.3.6

Maucci W (1991) Tre nuove specie di Eutardigradi della Groenlandia Meridionale. Bollettino del Museo Civico di Storia Naturale di Verona 15: 279–289.

Meyer HA, Hinton JG (2010) *Milnesium zsalakoae* and *M. jacobi*, two new species of Tardigrada (Eutardigrada: Apochela: Milnesiidae) from the southwestern United States. Proceedings of the Biological Society of Washington 123: 113–120. https://doi.org/10.2988/09-29.1

Michalczyk Ł, Kaczmarek Ł (2013) The Tardigrada Register: a comprehensive online data repository for tardigrade taxonomy. Journal of Limnology 72 (s1): 175–181. https://doi.org/10.4081/jlimnol.2013.s1.e22

Michalczyk Ł, Wełnicz W, Frohme M, Kaczmarek Ł (2012a) Redescriptions of three *Milnesium* Doyère, 1840 taxa (Tardigrada: Eutardigrada: Milnesiidae), including the nominal species for the genus. Zootaxa 3154: 1–20. https://doi.org/10.11646/zootaxa.3154.1.1

Michalczyk Ł, Wełnicz W, Frohme M, Kaczmarek Ł (2012b) Corrigenda of Zootaxa 3154: 1–20. Redescriptions of three *Milnesium* Doyère, 1840 taxa (Tardigrada: Eutardigrada: Milnesiidae), including the nominal species for the genus. Zootaxa 3393: 66–68. https://doi.org/10.11646/zootaxa.3393.1.6

Mironov SV, Dabert J, Dabert M (2012) A new feather mite species of the genus *Proctophyllodes* Robin, 1877 (Astigmata: Proctophyllodidae) from the Long-tailed Tit *Aegithalos caudatus* (Passeriformes: Aegithalidae): morphological description with DNA barcode data. Zootaxa 3253: 54–61. https://doi.org/10.11646/zootaxa.3253.1.2

Morek W, Gąsiorek P, Stec D, Blagden B, Michalczyk Ł (2016a) Experimental taxonomy exposes ontogenetic variability and elucidates the taxonomic value of claw configuration in *Milnesium* Doyère, 1840 (Tardigrada: Eutardigrada: Apochela). Contributions to Zoology 85(2): 173–200. https://doi.org/10.1163/18759866-08502003

Morek W, Michalczyk Ł (2020) First extensive multilocus phylogeny of the genus *Milnesium* (Tardigrada) reveals no congruence between genetic markers and morphological traits. Zoological Journal of the Linnean Society 188: 681–693. https://doi.org/10.1093/zoolinnean/zlz040

Morek W, Stec D, Gąsiorek P, Schill RO, Kaczmarek Ł, Michalczyk Ł (2016b) An experimental test of eutardigrade preparation methods for light microscopy Zoological Journal of the Linnean Society 178: 785–793. https://doi.org/10.1111/zoj.12457

Morek W, Suzuki AC, Schill RO, Georgiev D, Yankova M, Marley NJ, Michalczyk Ł (2019a) Redescription of *Milnesium alpigenum* Ehrenberg, 1853 (Tardigrada: Apochela) and a description of *Milnesium inceptum* sp. nov., a tardigrade laboratory model. Zootaxa 4586(1): 35–64. https://doi.org/10.11646/zootaxa.4586.1.2

Morek W, Stec D, Gąsiorek P, Surmacz B, Michalczyk Ł (2019b) *Milnesium tardigradum* Doyère, 1840: The first integrative study of interpopulation variability in a tardigrade species. Journal of Zoological Systematics and Evolutionary Research 57(1): 1–23. https://doi.org/10.1111/jzs.12233

Morek W, Blagden B, Kristensen RM, Michalczyk Ł (In press) The analysis of inter- and intrapopulation variability of *Milnesium eurystomum* Maucci, 1991 reveals high genetic divergence and a novel type of ontogenetic variation in the order Apochela. Systematics and Biodiversity. https://doi.org/10.1080/14772000.2020.1771469

Moreno-Talamantes A, Roszkowska M, García-Aranda MA, Flores-Maldonado JJ, Kaczmarek Ł (2019) Current knowledge on Mexican tardigrades with a description of *Milnesium cassandrae* sp. nov. (Eutardigrada: Milnesiidae) and discussion on the taxonomic value of dorsal pseudoplates in the genus *Milnesium* Doyère, 1840. Zootaxa 4691(5): 501–524. https://doi.org/10.11646/zootaxa.4691.5.5

Nelson D, Bartels PJ, Guil N (2018) Tardigrade ecology. In: Schill RO (Ed.) Water bears: the biology of tardigrades. Zoological Monographs 2: 163–210. https://doi.org/10.1007/978-3-319-95702-9_7

Nowak B, Stec D (2018) An integrative description of *Macrobiotus hannae* sp. nov. (Tardigrada: Eutardigrada: Macrobiotidae: *hufelandi* group) from Poland. Turkish Journal of Zoology 42(3): 269–286. https://doi.org/10.3906/zoo-1712-31

Pilato G (1981) Analisi di nuovi caratteri nello studio degli Eutardigradi. Animalia 8: 51–57.

Ramazzotti G (1962) Tardigradi del Cile – con descrizione di quattro nuove specie e di una nuova varieta. Atti della Società Italiana di Scienze Naturali e del Museo Civico di Storia Naturale in Milano 101: 275–287.

Rambaut A, Suchard MA, Xie D, Drummond AJ (2014) Tracer v1.6. http://beast.bio.ed.ac.uk/Tracer

Ronquist F, Huelsenbeck JP (2003) MrBayes 3: Bayesian phylogenetic inference under mixed models. Bioinformatics 19: 1572–1574. https://doi.org/10.1093/bioinformatics/btg180

Schuster RO, Nelson DR, Grigarick AA, Christenberry D (1980) Systematic criteria of the Eutardigrada. Transactions of the American Microscopical Society 99(3): 284–303. https://doi.org/10.2307/3226004

Stec D, Smolak R, Kaczmarek Ł, Michalczyk Ł (2015) An integrative description of *Macrobiotus paulinae* sp. nov. (Tardigrada: Eutardigrada: Macrobiotidae: *hufelandi* group) from Kenya. Zootaxa 4052: 501–526. https://doi.org/10.11646/zootaxa.4052.5.1

Stec D, Gąsiorek P, Morek W, Kosztyła P, Zawierucha K, Kaczmarek Ł, Prokop ZM, Michalczyk Ł (2016) Estimating optimal sample size for tardigrade morphometry. Zoological Journal of the Linnean Society 178: 776–784. https://doi.org/10.1111/zoj.12404

Stec D, Morek W, Gąsiorek P, Kaczmarek Ł, Michalczyk Ł (2017) Determinants and taxonomic consequences of extreme egg shell variability in *Ramazzottius subanomalus* (Biserov, 1985) (Tardigrada). Zootaxa 4208: 176–188. https://doi.org/10.11646/zootaxa.4208.2.5

Stec D, Morek W, Gąsiorek P, Michalczyk Ł (2018a) Unmasking hidden species diversity within the *Ramazzottius oberhaeuseri* complex, with an integrative redescription of the nominal species for the family Ramazzottiidae (Tardigrada: Eutardigrada: Parachela). Systematics and Biodiversity 16: 357–376. https://doi.org/10.1080/14772000.2018.1424267

Stec D, Roszkowska M, Kaczmarek Ł, Michalczyk Ł (2018b) *Paramacrobiotus lachowskae*, a new species of Tardigrada from Colombia (Eutardigrada: Parachela: Macrobiotidae). New Zealand Journal of Zoology 45(1): 43–60. https://doi.org/10.1080/03014223.2017.1354896

Surmacz B, Morek W, Michalczyk Ł (2019) What if multiple claw configurations are present in a sample? A case study with the description of *Milnesium pseudotardigradum* sp. nov. (Tardigrada) with unique developmental variability. Zoological Studies 58: 32. https://doi.org/10.6620/ZS.2019.58-32

Surmacz B, Morek W, Michalczyk Ł (2020) What to do when ontogenetic tracking is unavailable: a morphometric method to classify instars in *Milnesium* (Tardigrada). Zoological Journal of the Linnean Society 188: 797–808. https://doi.org/10.1093/zoolinnean/zlz099

Tumanov DV (2003) *Isohypsibius borkini*, a new species of Tardigrada from Tien Shan (Kirghizia) (Eutardigrada: Hypsibiidae). Genus 14: 439–441.

Tumanov DV (2005) Two new species of *Macrobiotus* (Eutardigrada, Macrobiotidae) from Tien Shan (Kirghizia), with notes on *Macrobiotus tenuis* group. Zootaxa 1043: 33–46. https://doi.org/10.11646/zootaxa.1043.1.3

Tumanov DV (2006) Five new species of the genus *Milnesium* (Tardigrada, Eutardigrada, Milnesiidae). Zootaxa 1122: 1–23. https://doi.org/10.11646/zootaxa.1122.1.1

Tumanov DV (2007) Three new species of *Macrobiotus* (Eutardigrada, Macrobiotidae, *tenuis*-group) from Tien Shan (Kirghizia) and Spitsbergen. Journal of Limnology 66: 40–48. https://doi.org/10.4081/jlimnol.2007.s1.40

Vaidya G, Lohman JD, Meier R (2011) SequenceMatrix: concatenation software for the fast assembly of multigene datasets with character set and codon information. Cladistics 27: 171–180. https://doi.org/10.1111/j.1096-0031.2010.00329.x

Wallendorf M, Miller WR (2009) Tardigrades of North America: *Milnesium alabamae* nov. sp. (Eutardigrada: Apochela: Milnesiidae) a new species from Alabama. Transactions of the Kansas Academy of Science 112: 181–186. https://doi.org/10.1660/062.112.0404

Young A, Chappell B, Miller W, Lowman M (2016) Tardigrades of the tree canopy: *Milnesium swansoni* sp. nov. (Eutardigrada: Apochela: Milnesiidae) a new species from Kansas, U.S.A. Zootaxa 4072(5): 559–568. https://doi.org/10.11646/zootaxa.4072.5.3

Zawierucha Z, Stec D, Lachowska-Cierlik D, Takeuchi N, Li Z, Michalczyk Ł (2018) High mitochondrial diversity in a new water bear species (Tardigrada: Eutardigrada) from mountain glaciers in central Asia, with the erection of a new genus *Cryoconicus*. Annales Zoologici 68: 179–201. https://doi.org/10.3161/00034541ANZ2018.68.1.007

Zeller C (2010) Untersuchung der Phylogenie von Tardigraden anhand der Genabschnitte 18S rDNA und Cytochrom c Oxidase Untereinheit 1 (COX I). MSc Thesis, Technische Hochschule Wildau, Germany.

## Supplementary material 1

### The relationships between body length and buccal tube length in *Milnesium berladnicorum*

Authors: Witold Morek, Bartłomiej Surmacz, Łukasz Michalczyk

Data type: Graph

Explanation note: Graph illustrating the relationships between the body length and buccal tube length of *Milnesium berladnicorum* Ciobanu, Zawierucha, Moglan & Kaczmarek, 2014, with clearly visible clusters corresponding to instars 1–3.

Link: https://doi.org/10.3897/zse.96.52049.suppl1

## Supplementary material 2

### Matrix of *Milnesium reductum* genetic distances

Authors: Witold Morek, Bartłomiej Surmacz, Łukasz Michalczyk

Data type: genetic distance matrix

Explanation note: Summary of haplotypes and the matrix of uncorrected p distances between the five *Milnesium reductum* Tumanov, 2006 populations analysed in this study.

Link: https://doi.org/10.3897/zse.96.52049.suppl2

## Supplementary material 3

### The relationships between body length and buccal tube length in *Milnesium almatyense*

Authors: Witold Morek, Bartłomiej Surmacz, Łukasz Michalczyk

Data type: Graph

Explanation note: Graph illustrating the relationships between the body length and buccal tube length of *Milnesium almatyense* Tumanov, 2006, with clearly visible clusters corresponding to instars 1–3.

Link: https://doi.org/10.3897/zse.96.52049.suppl3

## Supplementary material 4

### The relationships between body length and buccal tube length in *Milnesium reductum*

Authors: Witold Morek, Bartłomiej Surmacz, Łukasz Michalczyk

Data type: Graph

Explanation note: Graph illustrating the relationships between the body length and buccal tube length of *Milnesium reductum* Tumanov 2006, with clearly visible clusters corresponding to instars 1–3.

Link: https://doi.org/10.3897/zse.96.52049.suppl4